Advanced Composite Materials
Publication details, including instructions for authors and subscription information:
http://www.tandfonline.com/loi/tacm20

A basic study on the prediction of local material behavior of composite bone plate for metaphyseal femur fractures

Ji-Hun Bae [a], Seong-Hwan Yoo [a] & Seung-Hwan Chang [a]
[a] School of Mechanical Engineering, Chung-Ang University, 221, Huksuk-Dong, Dongjak-Gu, Seoul, 156-756, Republic of Korea
Version of record first published: 19 Oct 2012.

To cite this article: Ji-Hun Bae, Seong-Hwan Yoo & Seung-Hwan Chang (2012): A basic study on the prediction of local material behavior of composite bone plate for metaphyseal femur fractures, Advanced Composite Materials, 21:4, 345-356

To link to this article: http://dx.doi.org/10.1080/09243046.2012.736351

Advanced Composite Materials
Vol. 21, No. 4, August 2012, 345–356

A basic study on the prediction of local material behavior of composite bone plate for metaphyseal femur fractures

Ji-Hun Bae, Seong-Hwan Yoo and Seung-Hwan Chang*

School of Mechanical Engineering, Chung-Ang University, 221, Huksuk-Dong, Dongjak-Gu, Seoul 156-756, Republic of Korea

(*Received 13 January 2012; accepted 12 June 2012*)

This paper presents a method for estimating the local property changes and predicting the failure of composite materials experiencing large shear deformations during the draping process. This method was applied to the bone plate used for metaphyseal femur fractures because it has a complex geometry. The local property changes of fabric composites due to macro/microscopic deformations during the draping process were evaluated by various tests, and the results were used to predict the static/fatigue behaviors of the bone plate. This paper is expected to present useful information on the design of composite structures with complex geometries and their performance evaluation.

Keywords: shear deformation; draping; metaphysis; compressive strength; fatigue tests

1. Introduction

Fiber-reinforced composite materials have been widely used in automobile, aerospace, and medical equipment industries to replace metals because of their excellent mechanical properties, such as high specific strength and high specific modulus [1–3]. Fabric composites are especially suitable for forming complex structures with a double curvature, such as hemisphere structures and car bodies [4–5]. Applications of fabric composites are not limited to mechanical components, but are being expanded to the prostheses used for healing bone fractures [6–7]. Since existing composite bone plates, which have been mainly used to heal diaphyseal fractures, have simple shapes, the changes in fiber arrangement and microstructure of the material were negligibly small even after thermoforming. Therefore, the material properties of nondeformed specimens obtained by tensile and compressive tests were simply used in the finite element analysis of composite bone plates [8]. However, for the case of the bone plates used in healing metaphyseal fractures, as shown in Figure 1, the forming process of the composite bone plates involves large shear deformations of the fabric composite during the draping process because the great trochanter has irregular shape and high curvature. These large deformations induce changes in the stacking sequence and microstructure of the fabric composite, as a result, these changes give rise to mechanical property changes of the materials [4,9,10]. These mechanical property changes should be considered in the finite element analyses of composite bone plates to obtain more reliable results. Although some efforts have tried to consider the shear deformations of fabric composites during the draping process by

*Corresponding author. Email: phigs4@cau.ac.kr

ISSN 0924-3046 print/ISSN 1568-5519 online

http://dx.doi.org/10.1080/09243046.2012.736351
http://www.tandfonline.com

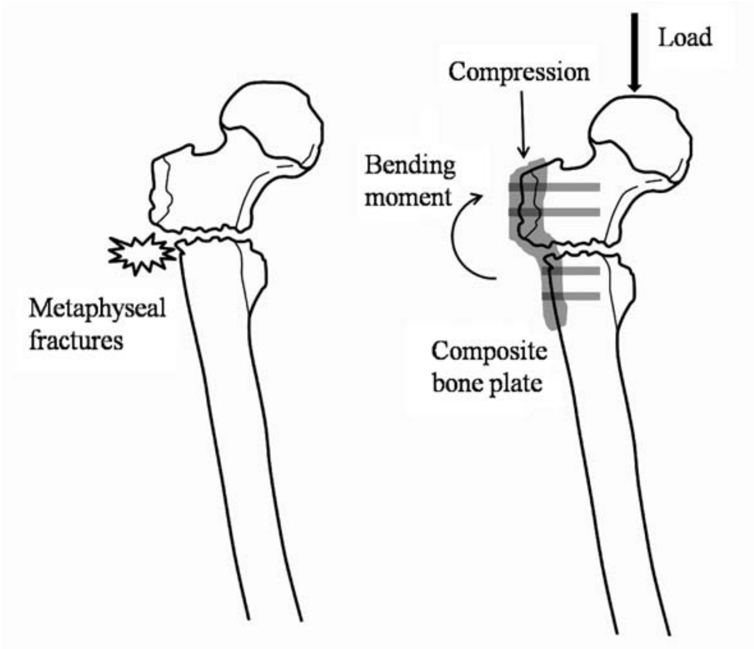

Figure 1. Metaphyseal femur fractures and bone plate application.

using nonorthogonal constitutive models, they were not able to consider microstructure changes, which induce changes in the local material property; therefore, they had a critical limitation in estimating the exact material properties and strength values [11].

In this paper, exact material property and strength of fabric composites deformed during the draping process were estimated by using several experimental tests, such as a draping test and a compressive test. The macroscopic shear deformation and the crimp angle variation of a fabric composite were measured and the two types of data were correlated. Compressive modulus, strength, and fatigue life according to shear angle were measured for specimens that experienced shear deformation through a picture frame test. By using the experimental results, the local material properties and fatigue life of the bone plate were estimated according to the shear angle generated by the draping process of the bone plate. This kind of basic research is expected to provide useful information on material deformation and property variation for more accurate analysis of a composite bone plate with complex geometry.

2. Specimen preparation

2.1. A picture frame test specimen

The plain weave carbon/epoxy prepregs (WSN3k, SK Chemicals, Korea) were used to prepare picture frame test specimens. The material properties are shown in Table 1. The biocompatibility of carbon/epoxy composite prosthetic devices has been already verified [12]. In order to fabricate sheared specimens with a certain amount of shear angle, 10 plies of prepregs of $290 \times 290\,\mathrm{mm}^2$ in size were stacked and then fixed to a picture frame rig. The picture frame rig was mounted on a universal testing machine (MTS 810, USA) and tensile load was applied at 1 mm/s in the z-direction to subject the fabric specimens (stacking sequence of $[45]_{10}$) to pure shear deformation, as shown in Figure 2. The relationship

Table 1. Material properties of carbon/epoxy prepregs.

	Plain weave	
Modulus [GPa]	Longitudinal (0°)	70
	Transverse (90°)	70
Ply thickness [mm]		0.23
Fiber volume fraction		0.6

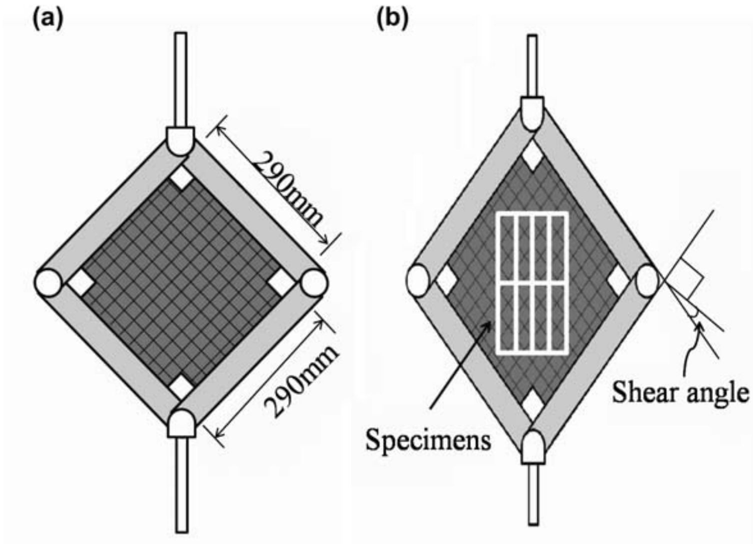

Figure 2. Picture frame test for prepreg deformation: (a) before shear deformation and (b) after shear deformation.

between the tensile load applied to the picture frame rig and the shear angle of the prepregs is shown in Figure 3, and this is a typical relationship of the picture frame and bias extension tests [13]. During the test, pure shear loads were imposed on the fabric specimens, whose clamped parts showed no signs of material slip and fiber tension due to misalignment.

2.2. Compressive test specimen

The prepregs that experienced pure shear deformation were cured in an autoclave by vacuum bag de-gassing molding and then several sheared specimens with various shear angles were cut from the center parts of the deformed specimens, respectively (see Figure 2(b)) to fabricate coupon type compressive test specimens, as shown in Figure 4. In order to prevent the cut specimens from generating microcracks at their edges during the water jet cutting process, all specimens were polished by an abrading paper (#400). The shear angles of the specimens were 16°, 26°, 34°, and 46°.

3. Experimental tests

3.1. Draping experiments

To determine the amount of local shear deformation that a composite bone plate undergoes, we draped the composite prepregs with a stacking sequence of $[45]_{10T}$ on a femur. The

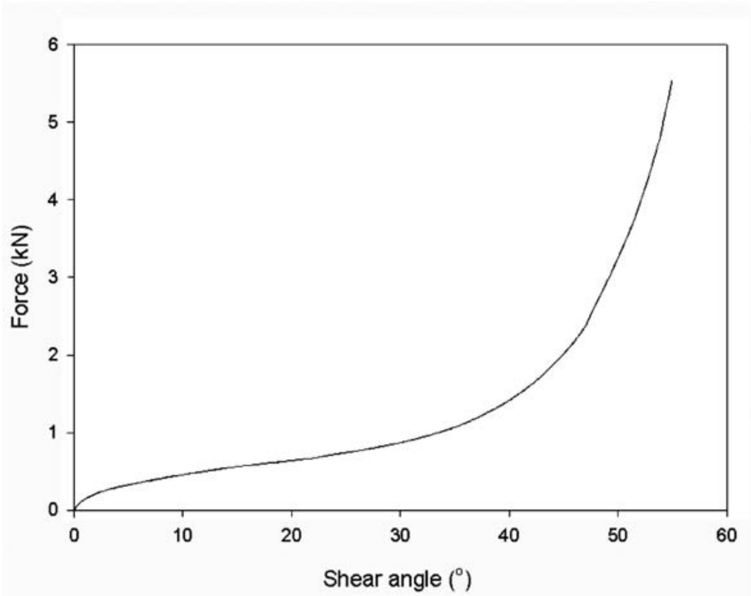

Figure 3. Force–shear angle curve of the fabric prepregs during the picture frame test.

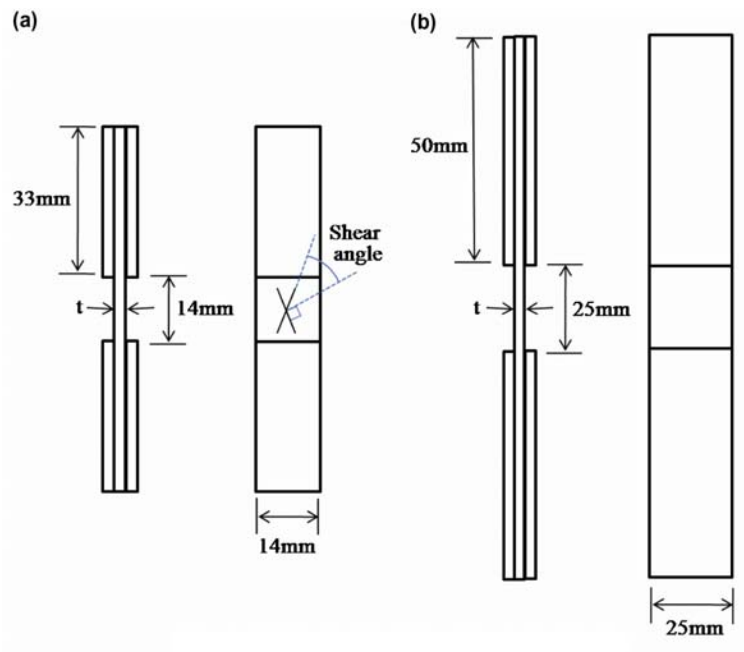

Figure 4. Fabric composite specimens: (a) static compression test and (b) fatigue test.

orthogonal directions along the fibers were marked on the prepreg (See Figure 5(a)) before the draping process to facilitate the observation of local shear deformation of the fabric composites on the metaphsis part. The draped femur, which was put in an external silicone

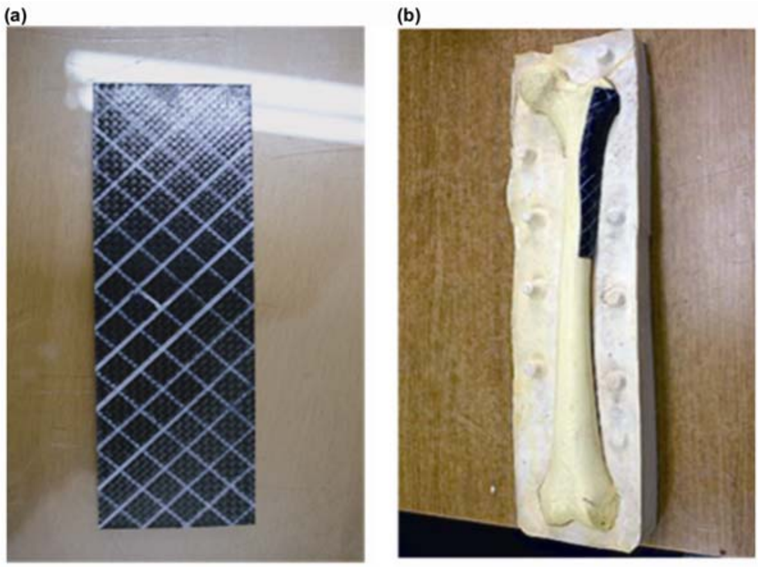

Figure 5. Draping of prepregs on the bone surface: (a) orthogonal grid lines and (b) draping and molding.

mold as shown in Figure 5(b), was cured in an autoclave by vacuum bag de-gassing molding. Considering the fact that heat does not transfer effectively to the prepregs due to the low thermal conductivity of the silicone mold, the forming time was set 2 h longer at the maximum temperature (125 °C) than the conventional forming time of the fabric composites (WSN3k).

3.2. Static compression test

The major functions of a bone plate are both stabilization of fractured bones and load transfer to support the compressive loads and bending moments induced by the body weight when a patient is walking (See Figure 1). Therefore, it is very important to estimate the compressive strength of the bone plate material according to shear angle to predict material failure. Since a coupon-type specimen can buckle during a compressive test, an anti-buckling jig was used in the test following ASTM D695 [14] at a strain rate of 1.3 mm/mm. As a result, the compressive modulus and strength of the fabric composite according to shear deformation increased because the fibers were rearranged in the direction of the load as the shear angle increased (See Figure 6) [9,10,15]. The compressive modulus of the fabric composite was similar to the result estimated by the classical laminate plate theory [16] considering only the stacking sequence of the composite laminate, which means that the chord modulus was not greatly affected by the microstructure of the fabric composite. However, the measured compressive strengths were less than the estimated strength of the unidirectional (UD) prepregs with the same fiber, matrix, and stacking angle as the fabric specimens, which was caused by the deformation of the microstructure of the fabric composites during shear deformation [9,10,15]. Crimp angle (See Figure 7) is known to influence the compressive properties of composites because it causes the composites to micro-buckle when compressive loads are applied [10,15,17]. In order to measure crimp angle changes with respect to the shear angle, the shear deformed composite laminate was cut along the longitudinal tows and the cross

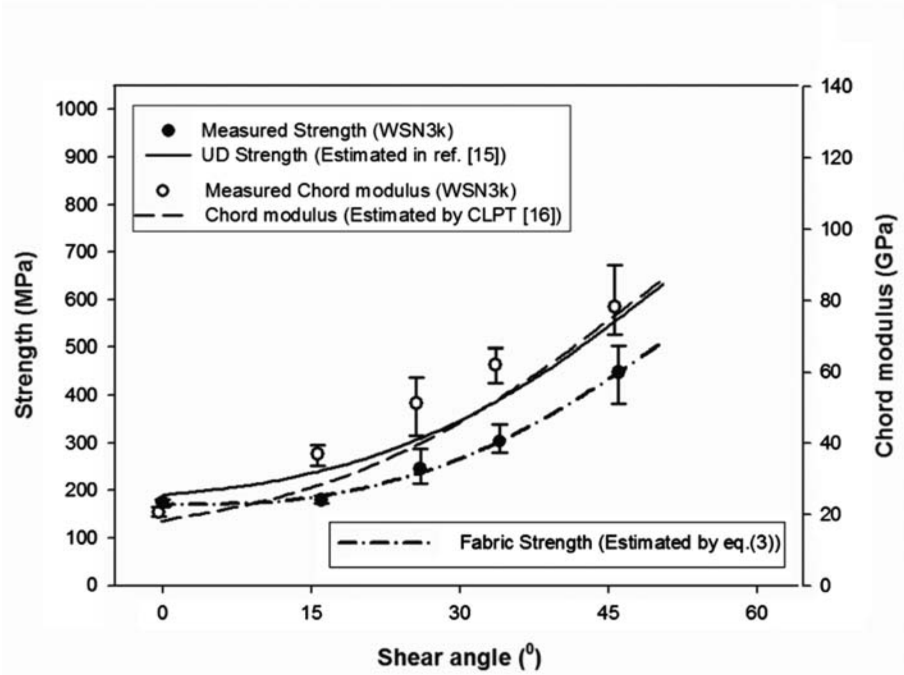

Figure 6. Chord moduli and compressive strengths of the sheared specimens.

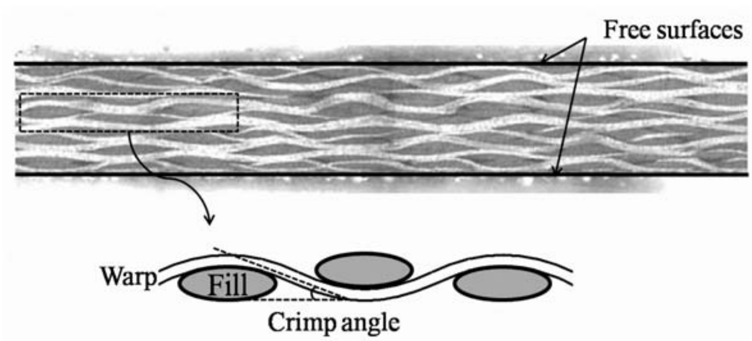

Figure 7. Micrograph of the tow structure of the fabric prepreg and its unit tow cell.

section was observed. The crimp angle was measured based on the free surfaces (upper/bottom flat surfaces: See Figure 7) of the specimen. More than 10 longitudinal tows were randomly selected to measure the crimp angle, and the measured crimp angles were averaged. The relationship between crimp angle and shear angle is shown in Figure 8. According to the observation results, the crimp angle increased linearly with the shear angle.

3.3. *Compression–compression fatigue test*

The specimens were mounted on a universal testing machine with hydraulic wedge grips in the compression–compression fatigue test, whose grip pressure was 10 MPa. The specimens

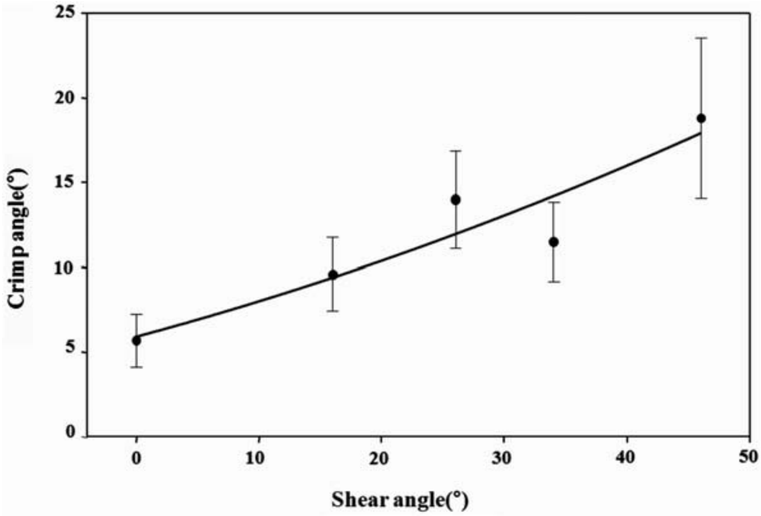

Figure 8. Correlation of crimp angle and shear angle.

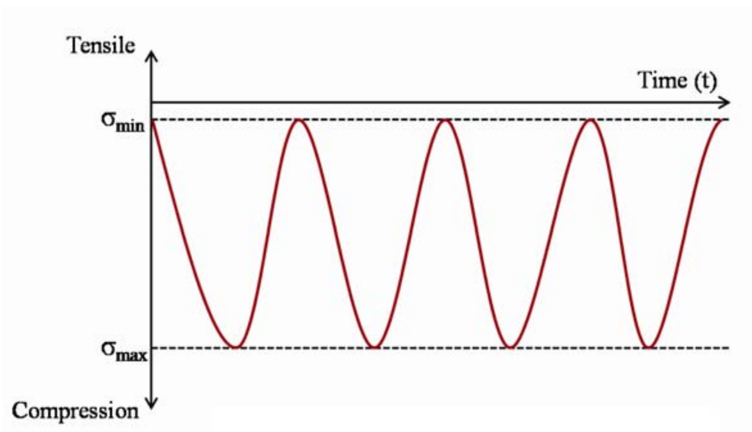

Figure 9. Loading cycle for fatigue tests.

were aligned in the direction of the compressive load by an alignment guide during the fatigue test. The load history and stress ratio applied for the fatigue test are illustrated in Figure 9. The fatigue test was carried out by using the load control method and the stress ratio (*R*) of the minimum stress to maximum stress was five. The load frequency was 8 Hz of a sinusoidal waveform. The load that was to be applied to a specimen was determined by multiplying the static compressive strength of the specimen and the normalized maximum stress to be applied (See Equation (1)).

$$r = \frac{\sigma_{\min}}{S_c} \tag{1}$$

where $\sigma_{\min}$ and S_c represent the minimum compressive stress to be applied to the specimen and the static compressive strength of the material, respectively. The fatigue life

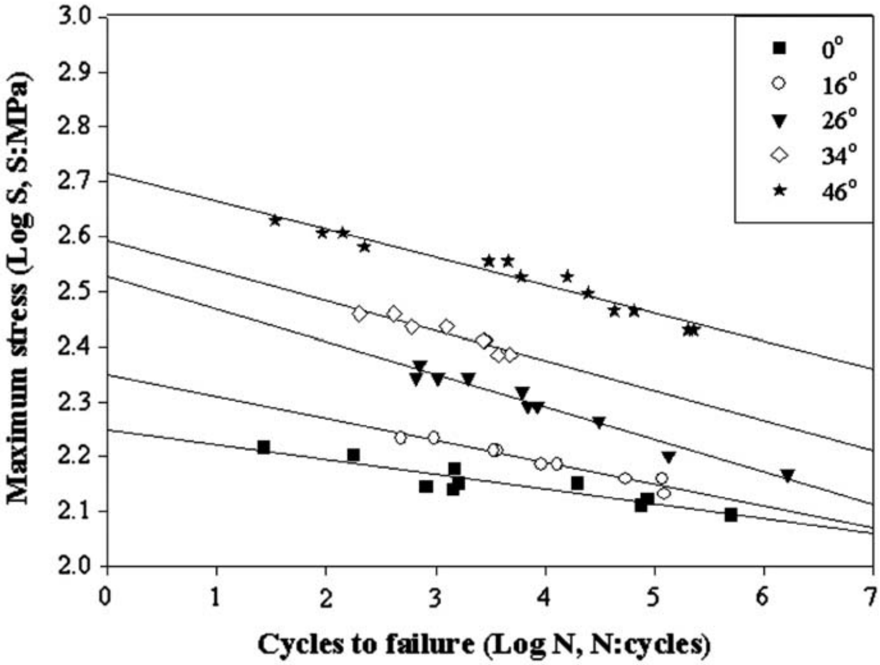

Figure 10. Fatigue life of sheared fabric specimens according to shear angle.

curve (log S–log N graph) according to the shear angle with corresponding normalized maximum stress was obtained as shown in Figure 10. This result can be used to predict the fatigue life of a composite bone plate under periodic loading of various amplitudes.

4. Prediction of local properties of composite bone plate

4.1. Local shear deformation

Shear angles at several positions in the bone plate were measured to determine the level of shear deformation of the draped bone plate. Since the level of shear deformation varied with the position in the bone plate, shear angles were measured mainly at the sites of relatively complex geometry. The shear deformation map is shown in Figure 11 and the corresponding shear angle at each position is listed in Table 2. High shear angles were concentrated on the greater trochanter having high double curvatures (A–D, 1–3, a–c in Figure 11), but shear deformation hardly occurred at the relatively simple-shaped diaphysis because of the simpler curvature.

4.2. Prediction of local property and fatigue life

Based on the observation results of the cross sections of the shear-deformed composite specimens, the relationship between shear angle (θ) and cramp angle (ρ) (Figure 8) is presented by Equation (2).

$$\theta = 3.84\rho - 21.43 \tag{2}$$

Figure 11. Shear deformation map.

Table 2. Shear angles at each position.

Position	Shear angle (°)	Position	Shear angle (°)
A	3	a	4
B	5	b	6
C	10	c	3
D	8	d	1
E	2	e	2
1	11	α	2
2	5	β	5
3	6	γ	5
4	1	δ	4
5	1	ε	4

By using the test results of the variation of compressive strength due to microstructure deformation (see Figure 6), the compressive strength of a woven composite with shear angle can be expressed by the following equation [15]:

$$S_{\text{sheared}} = \frac{E_\beta}{E_0} S_0 m^2 + \frac{E_\beta}{E_{45}} S_{45}(1 - m) - (8.17\rho - 25.76) \quad (3)$$

where S_0 and S_{45} are the compressive strengths of specimens $[0]_{16T}$ and $[\pm 45]_{4s}$ made of a UD carbon/epoxy composite (USN125, SK Chemical, Korea), respectively, and E_0 and E_{45} are the compressive moduli of specimens $[0]_{16T}$ and $[\pm 45]_{4S}$ made of a UD carbon/epoxy composite, respectively. E_β represents the compressive modulus of the specimen of $[\pm\beta]_{4S}$ made of a UD carbon/epoxy composite, which was calculated by the classical laminate plate theory [16], and m represents $\cos 2\beta$. The UD carbon/epoxy composite was composed of the same fiber and matrix system as the fabric composites (WSN3k) used in this research. The only difference between the two materials was the woven structure. This modified equation gave excellent predictions of the compressive strength of a fabric composite as shown in Figure 6.

Based on the proposed equation and measured data, the compressive properties of the fabric composites according to the position in the bone plate were calculated by classical laminate plate theory (CLPT) and Equation (3) as listed in Table 3. And these data were compared with those of the un-sheared specimen used as the reference data. Based on the result of Table 3, the compressive strength of the composite bone plate that experienced shear deformation during the draping process is illustrated as shown in Figure 12. All the compressive strengths illustrated in Figure 12 were limited to the axial values considering the loads applied to the bone plate (a compressive force and a bending moment; See Figure 1). As listed in Table 3, shear angle, crimp angle, compressive strength, etc. were changed according to the position in the bone plate, and the maximum and minimum static compressive strengths were 177.3 and 170.0 MPa, respectively. Assuming a patient walks at a speed of 2 Hz for 4 h a day during a healing period of 6 months, the repetitive loads of total 1,296,000 cycles would act on the fracture site. In order for the composite material not to get damaged during healing period, maximum stress (logs S) should not exceed 2.1 based on the fatigue data of the composites (Figure 10). Accordingly, if the bone plate receives fatigue stresses of less than approximately 100 MPa (in the case of $[45]_{10T}$), the bone plate would be safe from mechanical damage. This analysis will be evaluated more accurately by calculating the stress distributions of composite bone plates under actual loads.

Table 3. Local property variation of the draped bone plate according to position.

Position	Shear angle (°)	Crimp angle (°)	Modulus (GPa)	Strength (MPa)
Ref	0	5.57	15.5	170.6
A	3	6.36	16.9	170.0
B	5	6.87	17.9	170.6
C	10	8.18	20.9	175.6
D	8	7.66	19.6	172.9
E	2	6.10	16.4	170.1
1	11	8.44	21.5	177.3
2	5	6.87	17.9	170.6
3	6	7.14	18.4	171.1
4	1	5.84	16.0	170.3
5	1	5.84	16.0	170.3
a	4	6.61	17.3	170.2
b	6	7.14	18.4	171.1
c	3	6.36	16.9	170.0
d	1	5.84	16.0	170.3
e	2	6.10	16.4	170.1
α	2	6.10	16.4	170.1
β	5	6.87	17.9	170.6
γ	5	6.87	17.9	170.6
δ	4	6.61	17.3	170.2
ε	4	6.61	17.3	170.2

Figure 12. Strength distribution of bone plate.

Since the above results and the evaluation process of composite damage did not take into account material degradation due to prolonged exposure to *in vivo* environment, the composite materials should be tested under various environments to predict their fatigue characteristics more accurately and obtain more reliable data on their material properties. Furthermore, the variations of fatigue characteristics according to loading conditions (normal gait pattern is difficult in the early healing period and it becomes better with healing time) during the healing period should be considered to obtain more accurate results.

5. Conclusion

In this paper, the microstructural changes of a composite bone plate induced by local shear deformation of the fabric composites and their effect on the bone plate properties were experimentally evaluated by measuring the strength and modulus of fabric composites according to the shear angle. And the measured compressive behaviors of the composite materials were applied to the evaluation of the material behavior of the fabric composite bone plate draped on a femur. For this study, shear angles were measured at several major positions in the draped composite bone plate. And by using both the relationship between shear angle and crimp angle and the experimental results of material behavior according to shear angle obtained in preliminary studies [9,15], local Young's modulus, compressive strength, and fatigue life were evaluated. As a result, the composite bone plate had relatively large shear angle (maximum 11°) at the great trochanter having a complex geometry and at this position, the Young's modulus and compressive strength increased up to 38.7% and 3.9% (Position '1' in Figure 11), respectively, compared to the case of the un-sheared specimen. Even though the change in compressive strength was relatively small, the experimental findings of this research may be significant information that can help in the prediction of the exact deformation behavior and failure of a composite bone plate exposed to actual loading conditions. Such predictions of changes in material properties induced by local deformation can be used for the precise structural design of composite structures with complex geometries using finite element analysis.

Acknowledgment

This research was supported by the Mid-career Researcher Program through a National Research Foundation (Grant No. 2010-0009372) funded by the Ministry of Education, Science, and Technology of the Korean government.

References

[1] Bae JM. Fiber reinforced composite material. J. Korean Acad. Dent. Sci. 2009;47:17–24.
[2] Lee DG, Oh BK. Design and fabrication method of automobile composite components. J. Korean Soc. Automot. Eng. 1994;16:45–54.
[3] Song OS, Kim KT. A study on the aileron reversal characteristics of CAS composite aircraft wing. J. Korean Soc. Aeronaut. Space Sci. 2009;37:1192–1200.
[4] Sharma SB, Sutcliffe MPF, Chang SH. Characterisation of material properties for draping of dry woven composite material. Comp. Part A. 2003;34:1167–1175.
[5] Duflou JR, Moor JD, Verpoest I, Dewulf W. Environmental impact analysis of composite use in car manufacturing. CIRP Ann. Manuf. Technol. 2009;58:9–12.
[6] Kim SH, Chang SH, Jung HJ. The finite element analysis of a fractured tibia applied by composite bone plates considering contact conditions and time-varying properties of curing tissue. Compos. Struct. 2010;92:2109–2118.
[7] Huang ZM, Fujihara K. Stiffness and strength design of composite bone plates. Compos. Sci. Technol. 2005;65:73–85.
[8] Kim JH, Chang SH. A design on composite bone plate for fractures bone healing. J. Korean Soc. Compos. Mater. 2007;20:7–12.
[9] Kim SJ, Chang SH. The effect of micro-geometry of fabric composites on compressive characteristics. Proceeding of 8th International Conference on Textile Composites – TEXCOMP-8. Nottingham (UK); 2006
[10] Yoo SH, Park SW, Chang SH. Compressive characteristics of composites according to the micro-structure and stacking angle. J. Korean Soc. Compos. Mater. 2009;22:15–21.
[11] Hahn YW, Chang SH, Cheon SS. Finite element analysis of compression behavior of composite egg-box panel with non-orthogonal constitutive model. SAE Int. J. Mater. Manuf. 2009;2:352–357.
[12] Ramakrishna S, Mayer J, Wintermantel E, Leong KW. Biomedical applications of polymer-composite materials: a review. Compos. Sci. Technol. 2001;61:1189–1224.
[13] Lee WO, Um MK, Byun JH, Cao J. Characterization of in-plane shear behaviors of woven fabrics by bias-extension and trellis-frame tests. J. Korean Soc. Compos. Mater. 2010;23:8–14.
[14] ASTM D695-10. Standard test method for compressive properties of rigid plastics. United States: ASTM International; 2010.
[15] Yoo SH, Park SW, Chang SH. An experimental study on the effect of tow variations on compressive characteristics of plain weave carbon/epoxy composites under compressions. Compos. Struct. 2010;92:736–744.
[16] Lee DG, Suh NP, editors. Axiomatic design and fabrication of composite structures: applications in robots, machine tools, and automobiles. New York (NY): Oxford University Press; 2006.
[17] Yoo SH, Ho YG, Chang SH. A study on the compressive characteristics of co-cured foam-composite sandwich structures according to the crimp angle variations. Polym. Compos. 2009;30:1364–1370.